Solar PV Based Zeta Converter with Capacitor Multiplier and Coupled Inductor for DC Drive Application

G.Arthiraja, M. Ammal Dhanalakshmi, B.Arunkumaran and M. Sasikumar

Abstract— **in this paper performance of DC drive fed by high step-up converter is studied. High step up zeta converter is employed here with solar PV as a source without Extreme duty ratios and the numerous turns-ratios of a coupled inductor , converter achieves a high step-up voltage-conversion ratio and the leakage inductor energy of the coupled inductor is efficiently recycled to the load. These features explain the module's high efficiency performance. The operating principles and steady-state analyses of continuous and boundary conduction modes, as well as the voltage and current stresses of the active components, are analyzed for a 250W circuit model using MATLAB SIMULINK.**

Index Terms— **Zeta converter, PWM technique, Coupled Inductor, Active Switch.**

I. Introduction

In recent years photovoltaic (PV) has became attractive as a result PV market would grow up to 30 GW by 2014, due to the following policy-driven scenario [1];One type of renewable energy source is the photovoltaic (PV) cell, which converts sunlight to electrical current, without any form for mechanical or thermal interlink. Fig.1 Shows the block diagram of the proposed converter, that the PV panel (100~300W) is connected to the high step-up DC_DC converter, the input voltage of the converter is 15~40Volt from the PV panel.

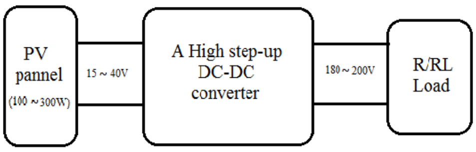

Fig.1 General configuration of DC module.

PV cells are usually connected together to make PV modules, consisting of 72 PV cells, which generates a DC voltage between 15 Volt to 45 Volt and a typical maximum power of 160 Watt, depending on temperature and solar irradiation. Fig. 2 shows that the maximum power point (MPP) voltage range is from 15 V to 40 V with various power capacities of about 100 W to 300 W for a single commercial PV panel.

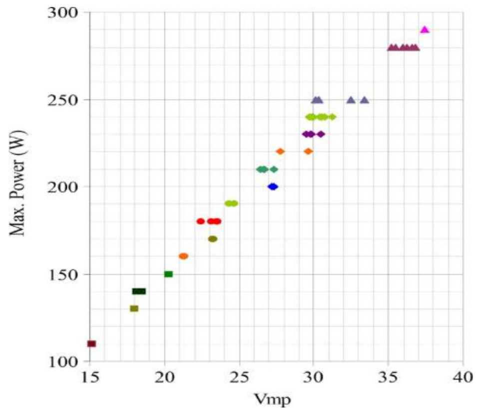

Fig.2 MPP voltage (V_{mp}) distribution with various power capacities of PVpanel.

The typical Zeta converter will provide either a step-up or a step-down function to the output, similar to that of the buck-boost or SEPIC converter topologies.The conventional Zeta converter has been configured of two inductors, a series capacitor and a diode. Previous research works have developed diverse Zeta converter applications, as follows.A coupled inductor could be employed to reduce power supply dimensions[2]. Some Zeta and fly back combination converters have extend the output range by the use of this coupled-inductor technique[3],[5].]. By Employing soft switching technique, zero-voltage switching and zero-current switching, on the Zeta converter; and hanging the input inductor of the ZETA converter[3],[6],[7]; to a coupled inductor have obtained a higher step-up conversion ratio[8],[20]. Many research works on high step-up converter topology included analyses of the switched-inductor and switched-capacitor types[9]–[11],transformerless switched-capacitor type [12], [13],the boost type integrated with the coupled inductor [14], [15], the voltage-lift type and the capacitor-diode voltage multiplier. The equivalent series resistance (ESR) of the capacitor and the parasitic resistances of the inductor are also affecting the overall efficiency. In regard to increasing voltage gain, this attribute is constricted by the voltage stress on the active switch. However, if the leakage inductor energy of the coupled inductor could be recycled, then the voltage stress is reduced on the active switch, that means the coupled-inductor and the voltage-multiplier or voltage-lift techniques are able to accomplish the goal of achieving higher voltage gain [2]–[22].The DC-DC boost converter is used for voltage step-up applications, and in this case this converter will be

Manuscript received November 29, 2013.

G.Arthiraja, PG Scholar, Dept. of Power Electronics and Drives, Jeppiaar engineering College, Chennai, India, 9677969377.

B. Arunkumaran, PG Scholar, Dept. of Power Electronics and Drives, Jeppiaar Engineering College, Chennai, India, 9445484322.

M. Ammal Dhanalakshm, PG Scholar, Dept. of Power Electronics and Drives, Jeppiaar Engineering College, Chennai, India, 9677282451.

M. Sasikumar, Professor & Head, Dept. of Power Electronics and Drives, Jeppiaar Engineering College, Chennai, India, 9094277053.

operated at extremely high duty ratio to achieve high step-up voltage gain. However, the voltage gain and the efficiency are limited due to the constraining effect of power switches, diodes, and the equivalent series resistance (ESR) of inductors and capacitors. Moreover, the extremely high duty-ratio operation will result in a serious reverse-recovery problem. Much higher voltage gain is achieved by using the coupled inductor and the voltage-multiplier or voltage-lift techniques. The operating principles and steady-state analysis are presented in the following sections.

II. OPERATING PRINCIPLES OF THE PROPOSED CONVERTERS

Fig. 3 shows the circuit configuration of the proposed converter, which consists of two active switch S1,one coupled inductor, three diodes D1~D3 and three capacitor C1~C3.The coupled inductor is modeled as a magnetizing inductor L_m, primary leakage inductor L_{k1}, secondary leakage inductor L_{k2}, and an ideal transformer.

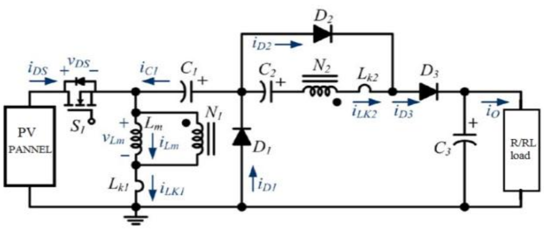

Fig.3 simplified model of proposed converter.

All components are ideal. The ON-state resistance RDS(ON) of the active switches, the forward voltage drop of the diodes, and the equivalent series resistance (ESR) of the coupled-inductor and output capacitors are ignored The turns ratio *n* of the coupled inductor *T*1 winding is equal to *N*2/*N*1.Fig. 4 shows some typical waveforms during one switching period in continuous conduction mode (CCM) operation. The operating principle and the five operating modes are described as follows.

A. CCM Operation

Mode I $[t_0, t_1]$: In this interval the capacitor C_2 obtain energy continuously from the secondary leakage inductor L_{k2}.The current flow path is shown in Fig. 5(a); switch S_1 and diodes D_2 are conducting. The source voltage V_{in} is applied on magnetizing inductor L_m and primary leakage inductor L_{k1} ,the current i_{Lm} is decreased; at the same time, L_m also releases its energy to the secondary winding, as well as charges the capacitor C_2 along with the decrease in energy, the charging current i_{D2} and i_{C2} also decreases. The secondary leakage inductor current i_{LK2} is being declined according to $i_{Lm/n}$. Once when the increasing i_{Lk1} equals the decreasing i_{Lm} this mode ends at $t=t_1$.

$$i_{in}(t) = i_{DS}(t) = i_{Lk1}(t) \quad (1)$$

$$\frac{di_{Lm}(t)}{dt} = \frac{v_{Lm}}{Lm} \quad (2)$$

$$\frac{di_{Lk1}(t)}{dt} = \frac{V_{in} - v_{Lm}}{L_{k1}} \quad (3)$$

$$i_{Lk2}(t) = i_{Lm}(t) - i_{Lk1}(t) \quad (4)$$

n

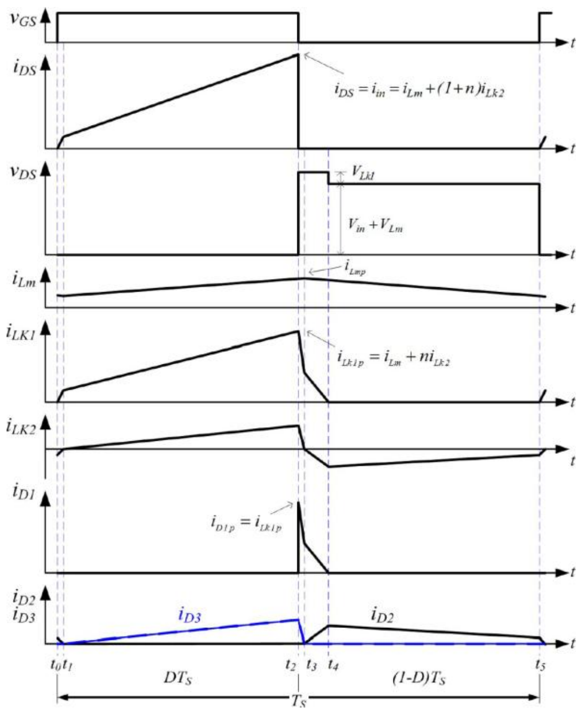

Fig.4. Typical waveforms of the proposed converter at CCM operation.

Mode II $[t_1, t_2]$: During this interval, source energy *Vin*is connected in series with C_1, C_2, secondary winding N_2, and L_{k2} to charge output capacitor C_3 and load *R*; at the same time, magnetizing inductor L_m also receives energy from V_{in}. The path of current flow is shown in Fig. 5(b); as illustrated, switch S_1remains on, and only diode D_3 is in conduction. The i_{Lm}, i_{Lk1}, and i_{D3} have been increasing because the V_{in} is crossing L_{k1}, L_m and primary winding N_1; L_m and L_{k1} are storing energy from V_{in}; as well as, $V_{in}$is also in series with N_2 of coupled inductor T_1, and capacitors C_1 and C_2 have been discharging their energy to capacitor C_3 and load *R*, that leads to increases in i_{Lm}, i_{Lk1}, i_{DS}, and i_{D3}. This mode ends at $t = t_2$ at which switch S_1 is turned off.

$$i_{Lm}(t) = i_{Lk1}(t) - ni_{Lk2}(t) \quad (5)$$

$$\frac{di_{Lm}(t)}{dt} = \frac{V_{in}}{Lm} \quad (6)$$

$$i_{in}(t) = i_{DS}(t) = i_{Lm}(t) + (1+n)\, i_{Lk2}(t) \quad (7)$$

$$\frac{di_{Lk2}(t)}{dt} = \frac{di_{D3(t)}}{dt} = \frac{(1+n)V_{in} + V_{C1} + V_{C2}}{Lk2} \quad (8)$$

Mode III $[t_2, t_3]$:During this transition interval, C_3 is being charged from secondary leakage inductor L_{k2} when switch *S*1 is turned off. The current flow path is shown in Fig. 5(c), and the diodes D_1 and D_3 are conducting. The energy stored in leakage inductor L_{k1} is flowing through diode D_1 and the capacitor C_1 is charged instantly when *S*1 turns off. Also, the L_{k2} keeps the same current direction as in the previous mode and is in series with C_2 to charge output capacitor C_3 and load *R*. The summation of V_{in}, V_{Lm}, and V_{Lk1} is the voltage across S_1. Currents i_{Lk1} and i_{Lk2} are rapidly declining, but i_{Lm} increases because $L_m$is receiving energy from L_{k2}. Once when the current i_{Lk2} drops to zero, this mode endsat$t = t_3$.

$$i_{in}(t) = 0 \quad (9)$$

$$i_{Lm}(t) = i_{Lk1}(t) - n i_{Lk2}(t) \quad (10)$$

$$\frac{di_{Lk1}(t)}{dt} = \frac{-V_{C1} - v_{Lm}}{Lk1} \quad (11)$$

$$\frac{di_{Lk2}(t)}{dt} = \frac{di_{D3(t)}}{dt} = \frac{n\, v_{Lm} + V_{C1} - V_o}{Lk2} \quad (12)$$

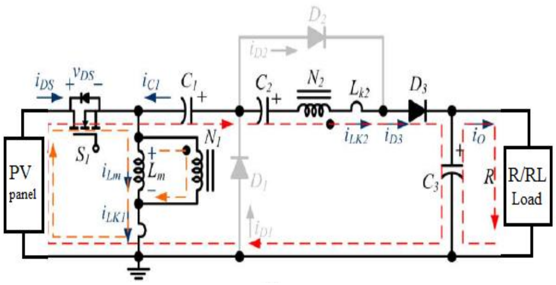

(a)

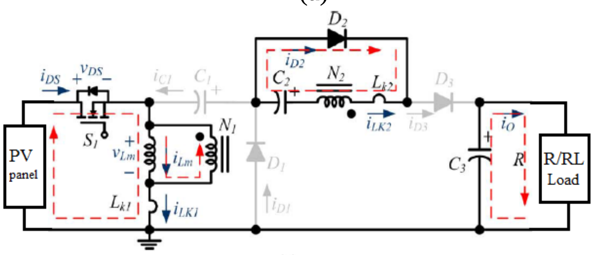

(b)

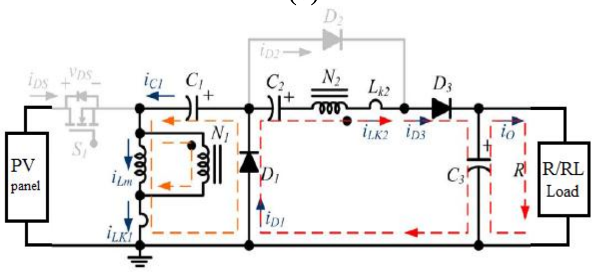

(c)

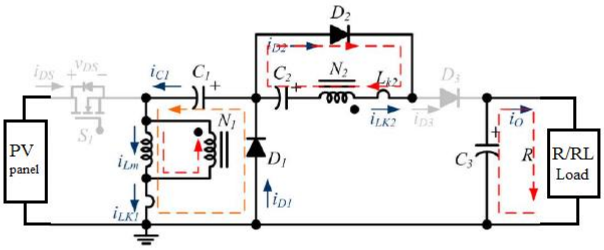

(d)

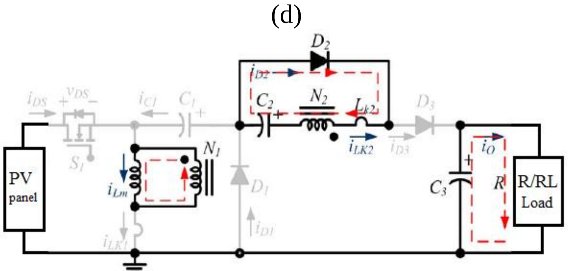

(e)Fig.5. During CCM operation, current flowing path in five modes operation (a) Mode I. (b) Mode II. (c) Mode III. (d) Mode IV. (e) Mode V.

Mode IV [t_3, t_4]:In this transition interval, the energy stored in magnetizing inductor L_m is released simultaneously to $C1$ and $C2$. The current flow path is shown in Fig. 5(d). and the diodes D_1 and D_2 are conducting. As leakage energy still flows through diode D_1 and continues to charge capacitor C_1,Currents i_{Lk1} and i_{D1} are persistently being decreased. Through T_1 and D_2 , the $L_m$is delivering its energy for charging capacitor C_2. The energy stored in capacitors C_3 is discharged constantly to the load R. The voltage across S_1 is the same as in the prior mode. Current i_{D2} is increasing but i_{Lk1} and i_{Lm} are decreasing, but. This mode ends when current i_{Lk1} becomes zero at $t = t_4$.

$$i_{Lm}(t) = i_{Lk1}(t) - n i_{Lk2}(t) \quad (13)$$

$$\frac{di_{Lk1}(t)}{dt} = \frac{-V_{C1} - v_{Lm}}{L_{k1}} \quad (14)$$

$$\frac{di_{Lk2}(t)}{dt} = \frac{n\, v_{Lm} + V_{C2}}{L_{k2}} \quad (15)$$

Mode V [t_4, t_5]:In this interval, magnetizing inductor L_m constantly transfers energy to C_2. The current flow path is shown in Fig. 5(e), and diode D_2 is alone conducting. Due to the continuous flow of magnetizing inductor energy through the coupled inductor T_1 to secondary winding N_2 and D_2 for charging capacitor C_2 the i_{Lm} is decreasing. The stored energy in capacitors C_3 constantly discharges to the load R. The summation of V_{in} and V_{Lm} is the voltage across S_1.When switch S_1 is turned on at the beginning of the next switching period this mode ends.

$$\frac{di_{Lm}(t)}{dt} = \frac{v_{Lm}}{Lm} \quad (16)$$

$$i_{Lk1}(t) = 0 \quad (17)$$

$$\frac{di_{Lk2}(t)}{dt} = \frac{n\, v_{Lm} + V_{C2}}{L_{k2}} \quad (18)$$

III. STEADY-STATE ANALYSIS OF PROPOSED CONVERTERS

CCM Operation:

To simplify the steady-state analysis, only modes II and IV are considered for CCM operation, and the primary & secondary side of leakage inductance are ignored. During mode II the following equations can be written,

$$v_{Lm} = V_{in}$$

$$vN_2 = nV_{in}$$

The following equations can be written from mode IV:

$$v_{Lm} = -V_{c1}$$

$$-vN_2 = V_{c2.}$$

Applying a volt-second balance on the magnetizing inductor Lm yields

$$\int_0^{DTS} (Vin)dt + \int_0^{DTS} (-V_{C1})dt = 0 \quad (19)$$

$$\int_0^{DTS} (nV_{in})dt + \int_0^{DTS} (-V_{C2})dt = 0 \quad (20)$$

the voltage across capacitor C_1 and C_2 are

$$V_{C1} = \frac{D}{1-D} V_{in} \quad (21)$$

$$V_{C2} = \frac{n\, DV_{in}}{1-D} \quad (22)$$

The output voltage V_o and the voltage gain M_{CCM} can be written as

$$V_O = V_{in} + \frac{DV_{in}}{1-D} + nV_{in} + \frac{nD\, V_{in}}{1-D} = \frac{(1+n)V_{in}}{1-D} \quad (23)$$

$$M_{CCM} = \frac{V_O}{V_{in}} = \frac{I_{in}}{I_O} = \frac{(1+n)}{1-D} \quad (24)$$

Fig. 6 shows voltage gain M_{CCM} as a function of duty ratio D by various turns ratios,and the turns ratio versus duty ratio under voltage gain of M_{CCM} = 8.

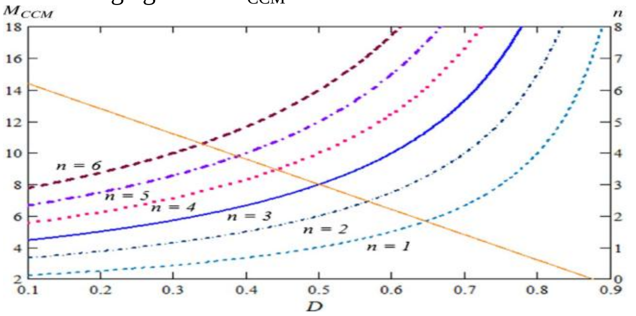

Fig.6. voltage gain M_{CCM} as function of duty ratio by various turns ratios, and the turns ratio versus duty ratio under voltage conversion is 8.

IV. DESIGN OF PROPOSED CONVERTER

The component parameter design and selection can be determined by following conditions,

A. Duty ratio (D): When the turns ratio n=3, that the duty ratio will be 75%.If the duty ratio is larger than 70%,conduction losses will be increased significantly. Thus, n=3 will be the correct choice for the duty ratio D=50%

B. Active Switch and Diodes: The voltage rating of the active switch can

$$V_{DS} = V_{D1} = \frac{V_O}{1+n} \quad (25)$$

$$V_{D2} = \frac{nV_O}{1+n} \quad (26)$$

$$V_{D3} = V_O \quad (27)$$

C. Magnetizing Inductor: By using the values of turns ratio and Duty ratio ,the converter are operated in BCM at 50 kHz operating frequency, The magnetizing inductance can be found as follows:

$$L_{mB} = \frac{f_s}{R_q} \cdot \frac{D^3 - 2D^2 + D}{2n^2 + 4n + 2} \quad (28)$$

D. Switched capacitor: The voltage of capacitor C_1 and C_2 could be obtained by (11)-(12) respectively ,The capacitance value are determined by

$$C_1 \geq \frac{2.\ P_{MAX}}{V^2_{C1}\ .f_s} \quad (29)$$

$$C_2 \geq \frac{2.\ P_{MAX}}{V^2_{C2}\ .\ f_s} \quad (30)$$

V. DISCUSSION OF SIMULATION RESULTS :

Operation of the proposed converter is illustrated using R and RL load. The performance is studied by using Matlab simulation. The simulink model of the proposed converter with R load and RL are shown in Fig.7.1 and Fig 7.2 respectively.

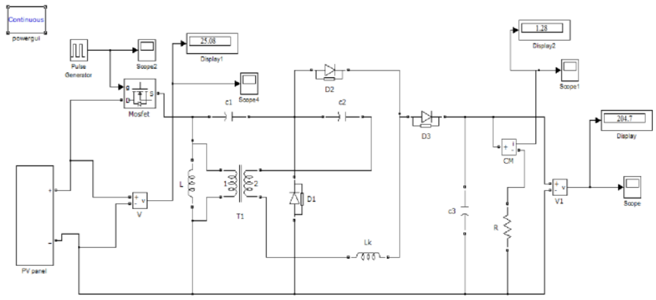

Fig.7.1 simulink model with R load.

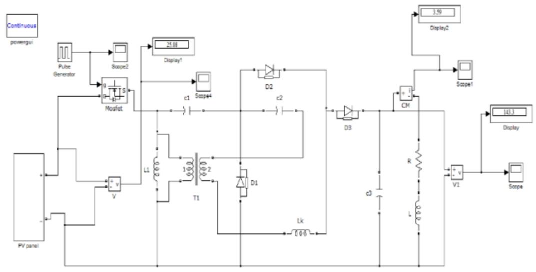

Fig.7.2 Simulink model with RL load

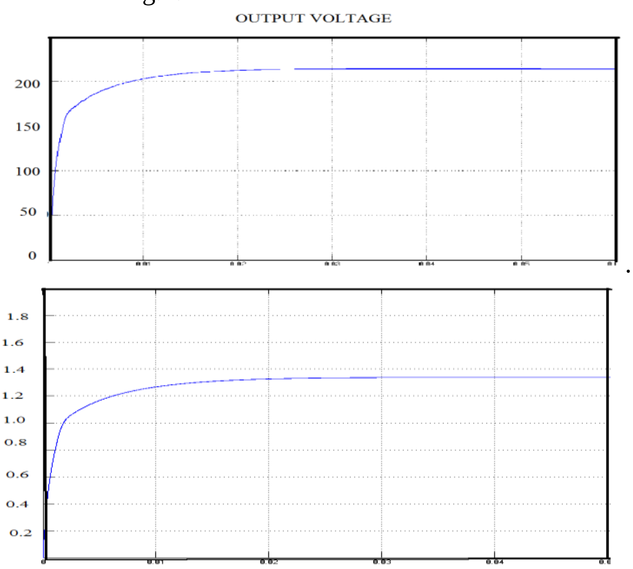

Fig.8.1 Output voltage and current for R load.

The resultant output voltage and output current is shown in fig. 8.1 and 8.2 respectively for both R and RL load.fig.9 shows the efficiency of the resistive load

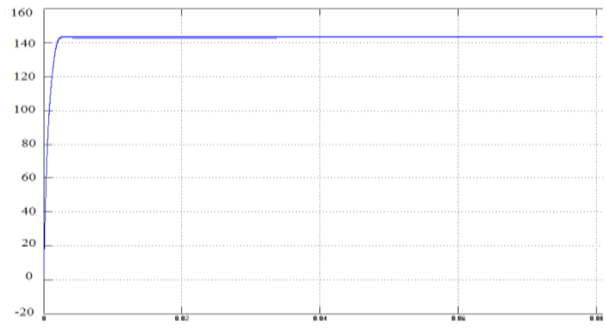

.

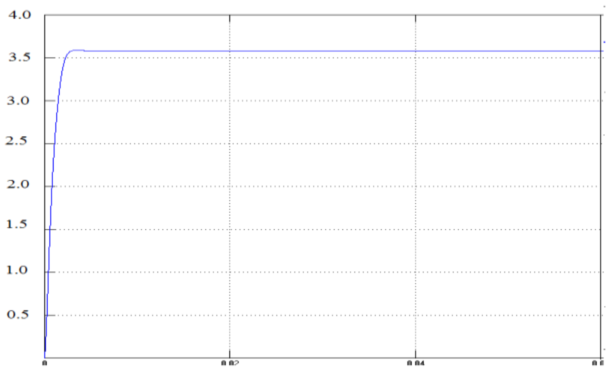

Fig.8.2 output voltage and current for RL load.

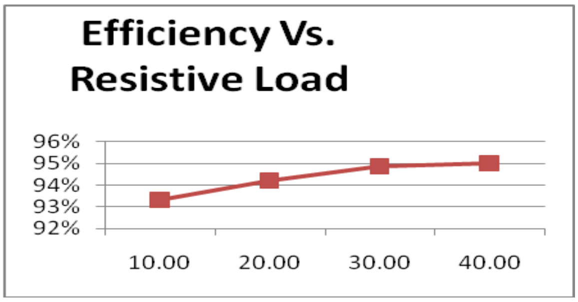

Fig.9 Efficiency versus resistive load.

VI. CONCLUSION

A high efficient DC/DC boost converter is proposed in this paper. The efficiency of the converter is improved by utilizing the energy stored in the coupled inductor and the two capacitors. Thus it makes the boost converter to implement in the drive applications. The experimental results prove that high voltage gain and efficiency are achieved. The results show that applying coupled-inductor turns ratio of $n = 3$ to the eight-times step-up voltage-conversion ratio attains maximum efficiency.

REFERENCES

[1] Global Market Outlook for Photovoltaics Until 2014, *Eur. PhotovoltaicInd. Assoc. (EPIA)*, Brussels, Belgium, May 2010. [Online]. Available:http://www.epia.org/fileadmin/EPIA_docs/public/Global_Market_Outlook_for_Photovoltaics_until_2014.pdf

[2] J. Falin, "Designing dc/dc converters based on ZETA topology,"*Analog Appl. J.*, pp. 16–21, 2Q, 2010. [Online]. Available: http://focus.ti.com/lit/an/slyt372/slyt372.pdf

[3] B. R. Lin and F. Y. Hsieh, "Soft-switching Zeta-flyback converter witha buck-boost type of active clamp," *IEEE Trans. Ind. Electron.*, vol. 54,no. 5, pp. 2813–2822, Oct. 2007.

[4] T. B. Marchesan, M. A. Dalla-Costa, J. M. Alonso, and R. N. do Prado,"Integrated Zeta-flyback electronic ballast to supply high-intensity dischargelamps," *IEEE Trans. Ind. Electron.*, vol. 54, no. 5, pp. 2918–2921,Oct. 2007.

[5] D. Murthy-Bellur and M. K. Kazimierczuk, "Two-transistor Zeta-flybackdc-dc converter with reduced transistor voltage stress," *Electron. Lett.*,vol. 46, no. 10, pp. 719–720, May 2010

[6] T. F. Wu, S. A. Liang, and Y. M. Chen, "Design optimization for asymmetricalZVS-PWM Zeta converter," IEEE Trans. Aerosp.Electron. Syst.,vol. 39, no. 2, pp. 521–532, Apr. 2003.

[7] R.Sudha,Ms.Ashly Mary Tom and M.Sasikumar (2012), 'An Efficient Non Isolated ZVT Boost Converter With A Single Resonant Inductor for Drive Applications,' International Journal of Knowledge Engineering and Research, Vol.1, Issue 2 , Pp. 76-80.

[8] B. Axelrod, Y. Berkovich, S. Tapuchi, and A. Ioinovici, "Steep conversionration C´ uk, Zeta, and sepic converters based on a switchedcoupled-inductor cell," in Proc. IEEE Power Electron. Spec. Conf., 2008,pp. 3009–3014.

[9] B.Axelrod, Y.Berkovich,and A.Ioinovici,"Switched-capacitor/switched-inductor structures for getting transformerless hybrid dc-dc PWM converters," IEEE Trans. Circuits Syst. I, Reg. Papers, vol. 55, no. 2,pp. 687–696, Mar. 2008.

[10] F. L. Luo, "Switched-capacitorized dc/dc converters," in Proc. IEEEICIEA, 2009, pp. 1074–1079.

[11] B. Axelrod, Y. Berkovich, and A. Ioinovici, "Transformerless dc-dc converterswith a very high dc line-to-load voltage ratio," in Proc. IEEEISCAS, 2003, vol. 3, pp. 435–438.

[12] L. S. Yang, T. J. Liang, and J. F. Chen, "Transformerless dc-dc converterswith high step-up voltage gain," IEEE Trans. Ind. Electron., vol. 56, no. 8,pp. 3144–3152, Aug. 2009.

[13] Q. Zhao and F. C. Lee, "High-efficiency, high step-up dc-dc converters,"IEEE Trans. Power Electron., vol. 18, no. 1, pp. 65–73, Jan. 2003.

[14] L. S. Yang, T. J. Liang, H. C. Lee, and J. F. Chen, "Novel highstep-up dc-dc converter with coupled-inductor and voltage-doubler circuits,"*IEEE Trans. Ind. Electron.*, vol. 58, no. 9, pp. 4196–4206,Sep. 2011.

[15] H.-L. Do, "Zero-voltage-switching synchronous buck converter with acoupled inductor," *IEEE Trans. Ind. Electron.*, vol. 58, no. 8, pp. 3440–3447, Aug. 2011.

[16]G.S Arunvishnu, S.Sellakumar and M.Sasikumar (2012),'Simulation and implementation of Variable Duty Cycle Control to Achieve High Input Power Factor for DCM Boost PFC Converters" International Journal of Engineering Research and Applications (IJERA), Vol. 2, Issue 2, Pp.138-141.

[17].F. Max Savio, R. Hemantha Kumar and M. Sasikumar (2013), "Power Optimisation and Performance Evolution of High Step-Up Solar PV System For Dc Drives", International Journal of Advanced Research in Electrical, Electronics and Instrumentation Engineering (IJAREEIE),Vol. 2, Issue 10, October 2013.

G. Arthiraja is currently pursuing Master of Engineering in Power Electronics and Drives in Jeppiaar Engineering College, Anna University, Chennai, Tamilnadu. Earlier he received his B.E degree in Electrical and electronics Engineering in Sri Sairam Engineering college, Anna University, Chennai in 2012. His current research interests include Renewable Energy Sources and DC-DC Converters.

M. Ammal Dhanalakshmi is currently pursuing Master of Engineering in Power Electronics and Drives in Jeppiaar Engineering College, Anna University, Chennai, Tamilnadu. Earlier she received her B.E degree in Elecrtrical and Electronics Engineering in Vel's Srinivasa college of engineering and technology, Chennai in 2009. Her current research interests include soft switching DC-DC Converters. She is a life member of ISTE.

B. ArunKumaran is currently pursuing Master of Engineering in Power Electronics and Drives in Jeppiaar Engineering College, Anna University, Chennai, Tamilnadu. Earlier he received his B.E degree in Electronics and Instrumentation Engineering in Thangavelu Engineering college, Anna University, Chennai in 2011. His current research interests includes Renewable Energy Sources and DC-DC Converters.

Dr.M.Sasikumar has received the Bachelor degree in Electrical and Electronics Engineering from K.S.Rangasamy College of Technology, Madras University, India in 1999, and the M.Tech degree in power electronics from VIT University, in 2006. He has obtained his Ph.d. degree from Sathyabama University, Chennai. Currently he is working as a Professor and Head in Jeppiaar Engineering College, Chennai Tamilnadu, India. He has published papers in National, International conferences and journals in the field of power electronics and wind energy conversion systems. His area of interest includes in the fields of wind energy systems and power converter with soft switching PWM schemes. He is a life member of ISTE.